N90-28267

# A COMPARISON OF ISCCP AND FIRE SATELLITE CLOUD PARAMETERS

Gary G. Gibson, Patrick W. Heck, David. F. Young
Aerospace Technologies Division, Planning Research Corporation
Hampton, Virginia 23666

Patrick Minnis and Edwin F. Harrison
Atmospheric Sciences Division, NASA Langley Research Center
Hampton, Virginia 23665-5225

## 1. Introduction

One of the goals of the First ISCCP Regional Experiment (FIRE) is the quantification of the uncertainties in the cloud parameter products derived by the International Satellite Cloud Climatology Project (ISCCP). This validation effort has many facets including sensitivity analyses (Rossow et al., 1989) and comparisons to similar data or theoretical results with known accuracies. The FIRE provides cloud-truth data at particular points or along particular lines from surface and aircraft measurement systems. Relating these data to the larger, area-averaged ISCCP results requires intermediate steps using higher resolution satellite data analyses. Errors in the cloud products derived with a particular method can be determined by performing analyses of high-resolution satellite data over the area surrounding the point or line measurement. This same analysis technique may then be used to derive cloud parameters over a larger area containing similar cloud fields. It is assumed that the uncertainties found for the small-scale analyses are the same for the large scale so that the method has been "calibrated" for the particular cloud type; i.e., its accuracy is known. Differences between the large-scale results using the ISCCP technique and the "calibrated" method can be computed and used to determine if any significant biases or rms errors occur in the ISCCP results. In this paper, selected ISCCP results are compared to cloud parameters derived using the hybrid bispectral threshold method HBTM (Minnis et al., 1987) over the FIRE IFO and extended observation areas.

## 2. Stratocumulus

GOES-West ISCCP B3 data taken every 3 hours during July 17-31, 1983 analyzed with the HBTM on a 2.5° latitude-longitude grid between 40°N and 10°N and 145°W and 110°W (Minnis et al., 1988) are compared to the corresponding C1 (Rossow et al., 1988) results. The cloud data have been stratified as total, low, midlevel, and high clouds. The ISCCP low, middle, and high clouds are those with cloud-top pressures $p > 800$ mb, $800 \text{ mb} \geq p > 440$ mb, and $p \leq 440$ mb, respectively. HBTM low, middle, and high clouds are those with cloud-top altitudes, $z < 2$ km, $2 \text{ km} \leq z < 6$ km, and $z \geq 6$ km. There are two primary types of ISCCP cloud cover, VIR, determined with visible and infrared data, and IR, determined with infrared-data alone. The two cloud amounts are the same at night. As noted by Minnis et al. (1988), the cloud amounts, diurnal cloud variations, and cloud-top heights do not vary dramatically on an interannual basis over this area. Also, the cloud properties derived from the satellite near the coast are very much like those determined over the open ocean within this grid. Thus, the large-scale average properties derived for this region are similar to those determined over smaller areas. Initial validations of the HBTM are described elsewhere (e.g., Minnis and Harrison, 1984; Minnis and Wielicki, 1988; and Minnis et al. (1989a,b).

Figure 1 shows the mean HBTM-derived total, low, and sum of middle and high cloud amounts. Total and low cloud amounts increase from the California coast to a maximum of 91% near 20°N, 130°W with a relative maximum in low cloudiness within the IFO region. This extensive cover of low clouds is referred to as the main stratocumulus region. Significant amounts of upper-level clouds occur in the southeastern quadrant of the grid. Differences between the HBTM and VIR results are shown in Fig. 2, while the HBTM-IR differences are plotted in Fig. 3. Neglecting the land areas, the mean VIR total cloud amounts (Fig. 2a) are 2 ± 6% greater than the HBTM values. Most of the ISCCP clouds, however, are placed in the middle layer as seen in the differences in Figs. 2b and 2c. More clouds are found with the HBTM over the main stratocumulus region than with the IR results. The IR underestimates total cloudiness by 7 ± 11%.

The differences in the 3-hourly means are examined in Fig. 4 for two large regions outlined in heavy lines in Fig. 1c. The western box is designated the PAC region, while the other is the IFO region. Over the PAC region (Fig. 4a), there is generally good agreement between the results for all three analysis techniques. The HBTM cloudiness is very close to the IR results during the day but greater at night. Addition of the visible data increases the ISCCP cloud amounts so the VIR cloud cover exceeds the HBTM amounts during the day. On average, the HBTM and IR cloud amounts are the same, while the VIR cloudiness is greater than the HBTM's. This tendency for slight daytime overestimation by the VIR technique (relative to the HBTM) and underestimation with the IR method is accentuated near the coast over the IFO region (Fig. 4b). There, the IR diurnal range is much smaller than the HBTM's with a 20% underestimate in total cloudiness at night and more than 10% during the day. The VIR data only underestimate the cloud cover during the night leading to an overall cloud amount deficit of 10%.

The overestimation of ISCCP cloud-top heights over the stratocumulus region is probably due to the use of low-resolution NMC soundings over areas with strong boundary-layer inversions (Minnis et al., 1989b). The VIR cloud amounts agree quite well with the HBTM results primarily because of the effects of underestimation at night and overestimation during the day. This result is consistent with the Landsat analyses of Parker and Wielicki (1989). The differences between the results over the PAC and FIRE regions are attributable to the variations in contrast between the clear-sky and cloudy temperatures. Near the coast, the clouds are lower than those further west so fewer pixels are cold enough to pass the 3-K threshold. Diurnal variations in cloud amount determined with either the VIR or IR techniques should be used carefully. While both techniques appear to give the correct times for maximum and minimum cloudiness, there may be significant discrepancies in the diurnal ranges and the variations in cloudiness between the extrema.

## 3. Cirrus

Another method for validating an algorithm is to apply it directly to a high-resolution satellite data set corresponding to a cloud-truth set. The complete ISCCP algorithm was not available for this study so an attempt is made here to simulate its relevant characteristics. The adjustment of cloud-top temperature to account for the infrared semi-transparency relies on a relationship between the visible and infrared optical depths, $\tau_v$ and $\tau_e$, respectively. In the ISCCP algorithm, $\tau_v = 2\tau_e$ (Rossow et al., 1988). The value of $\tau_v$ is determined from the observed reflectance by first isolating the cloud reflectance by accounting for the surface and atmospheric contributions to the reflectance. The cloud reflectance is related to $\tau_v$ using the results of a radiative transfer model of clouds based on a scattering phase function determined from Mie theory using a droplet size distribution with an equivalent radius of 10 $\mu$m. Once the value of $\tau_v$ is determined, the observed cloud temperature for a given pixel is adjusted in the same manner used by Heck et al. (1989). The corrected temperature is then compared to the tropopause temperature and, if lower, set to the tropopause value. The temperatures or corresponding pressures for each pixel are then averaged for the area of interest to obtain an average cloud-top temperature or altitude.

The approach of Heck et al. (1989) is used here with some modifications to simulate the ISCCP cloud-height adjustment scheme. Instead of an empirical cloud bidirectional reflectance model, a $\tau_v$-dependent model is used here which was constructed from the results of an adding-doubling model of radiative transfer (Takano and Liou, 1989) using a Mie-scattering phase function determined for a droplet distribution with an effective radius of 10 $\mu$m. The temperature of each cloudy pixel is adjusted individually using $\tau_v = 2\tau_e$. Averages are constructed from the adjusted pixel temperatures. Otherwise, all other steps are the same as those used by Heck et al. (1989). This simulated ISCCP algorithm was then applied to the lidar-satellite data used by Heck et al. (1989). The lidar-derived cloud-top heights are used as a reference set in the same manner used by Heck et al. (1989) to determine uncertainties in the results from the empirical method.

Comparisons of the simulated ISCCP cloud-top heights and the lidar cloud-center and cloud-top altitudes are shown as crosses in Figs. 5a and 5b, respectively. On average, the simulated ISCCP cloud-top heights are 2.8 km lower than the lidar cloud-center heights and 4.7 km lower than the lidar cloud-top altitudes. The range of differences leads to a large rms error of 3.4 km in the cloud-center height comparison. Average cloud heights for the 2.5° region bounded by 42.5°N and 45°N and 87.5°W and 90°W are also shown in Fig. 5 as circles. The ISCCP adjusted cloud-top heights are taken from the GOES C1 data for October 27 and 28, 1986. Averages from the 0.5° regional results of Heck et al. (1989) are used as the reference heights. The two lower cloud heights were observed on the 27th. The other three cases fall within the envelope of simulated data. Without the two low-level clouds, the observed ISCCP cloud-top heights are 1.7 km lower than the reference cloud-center heights and 2.5 km lower than the cloud-top heights.

The results shown in Fig. 5 demonstrate some consistency between the simulated and actual ISCCP cloud-top height results for semitransparent cirrus. Other cirrus IFO studies have indicated that the Mie scattering phase function is not a good representation of scattering in cirrus clouds. These preliminary findings support those conclusions.

## REFERENCES


Heck, P. W., G. G. Gibson, P. Minnis, and E. F. Harrison, 1989: Satellite derived cloud fields during the FIRE IFO case study. Presented at FIRE Annual Meeting/ASTEX Workshop, Monterey, CA, July 10-14.

Minnis, P., and E. F. Harrison, 1984: Diurnal variability of regional cloud and clear-sky radiative parameters derived from GOES data, Part I: Analysis method. J. Clim. Appl. Meteor., **23**, 993-1011.

Minnis, P., E. F. Harrison, and G. G. Gibson, 1987: Cloud cover over the eastern equatorial Pacific derived from July 1983 ISCCP data using a hybrid bispectral threshold method. J.Geophys. Res., **92**, 4051- 4073.

Minnis, P., and B. A. Wielicki, 1988: Comparison of cloud amounts derived using GOES and Landsat data. J. Geophys. Res., **93**, 9385-9403.

Minnis, P., E. F. Harrison, and D. F. Young, 1988: Extended time observations of California marine stratocumulus from GOES for July 1983-1987. FIRE Science Team Workshop, Vail, CO, July 11-15, 195-199.

Minnis, P., C. W. Fairall, and D. F. Young, 1989a: Intercomparisons of GOES-derived cloud parameters and surface observations over San Nicolas Island. Presented at FIRE Annual Meeting/ASTEX Workshop, Monterey, CA, July 10-14.

Minnis, P., D. F. Young, R. Davies, M. Blaskovic, and B. A. Albrecht, 1989b: Stratocumulus cloud height variations determined from surface and satellite measurements. Presented at FIRE Annual Meeting/ASTEX Workshop, Monterey, CA, July 10-14.

Parker, L., and B. A. Wielicki, 1989: Comparison of satellite based cloud retrieval methods. Presented at FIRE Annual Meeting/ASTEX Workshop, Monterey, CA, July 10-14.

Rossow, W. B., L. C. Garder, P. Lu, and A. Walker, 1988: International Satellite Cloud Climatology Project (ISCCP), Documentation of cloud data. WCRP Report, August, 78 pp.

Rossow, W. B., L. C. Garder, and A. A. Lacis, 1989: Global, seasonal cloud variations from satellite radiance measurements. Part I: Sensitivity of analysis. J. Clim., **2**, 419-418.

Takano, Y. and K. N. Liou, 1989: Radiative transfer in cirrus clouds: I. Single scattering and optical properties of oriented hexagonal ice crystals. J. Atmos. Sci., **46**, 3-20.

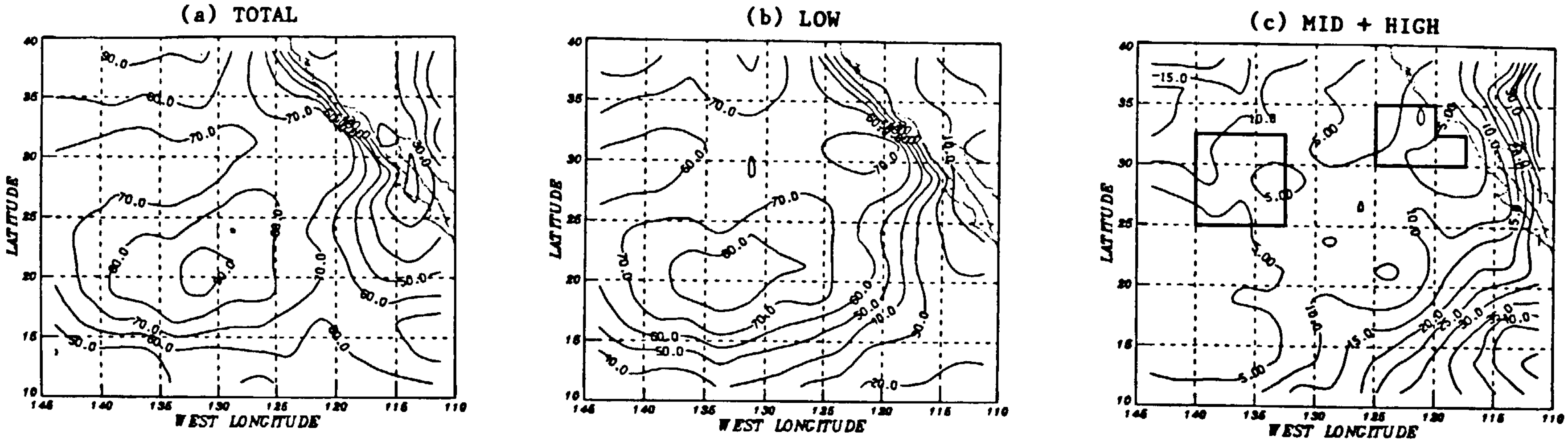


Fig. 1. Cloud amounts (%) derived with HBTM for July 17-31, 1983.

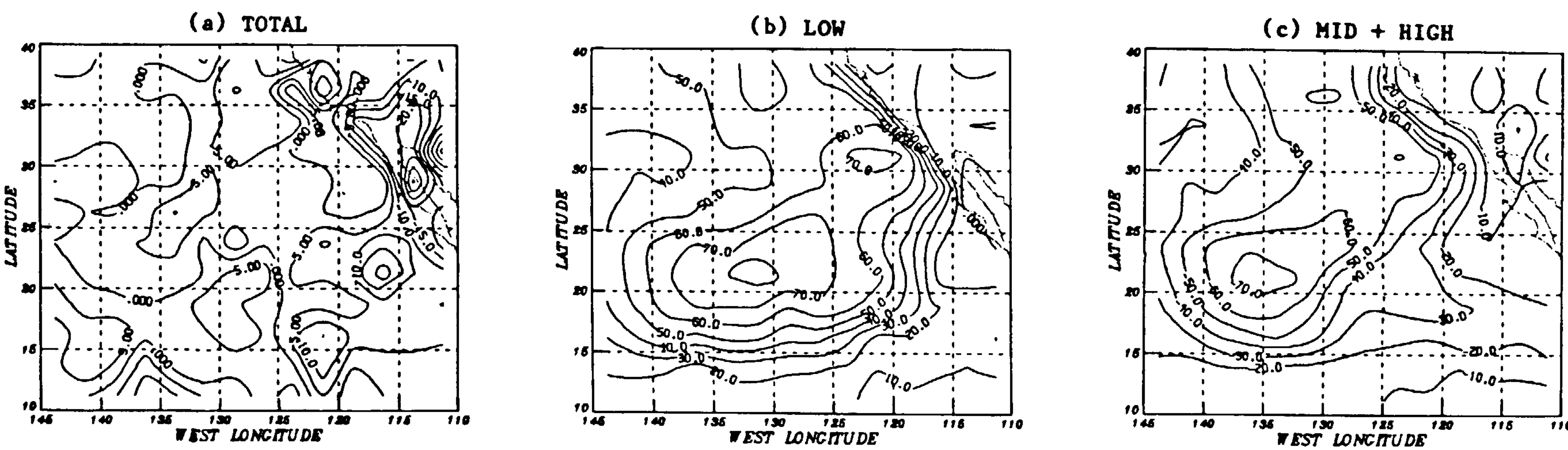


Fig. 2. Differences between HBTM and VIR cloud amounts (%) for July 17-31, 1983.

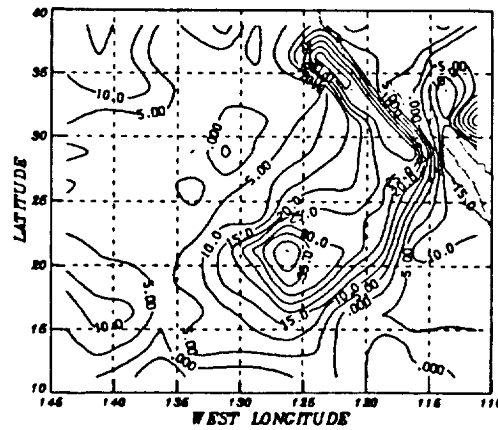


Fig. 3. Same as Fig. 2 except for HBTM
and IR total cloud amounts.

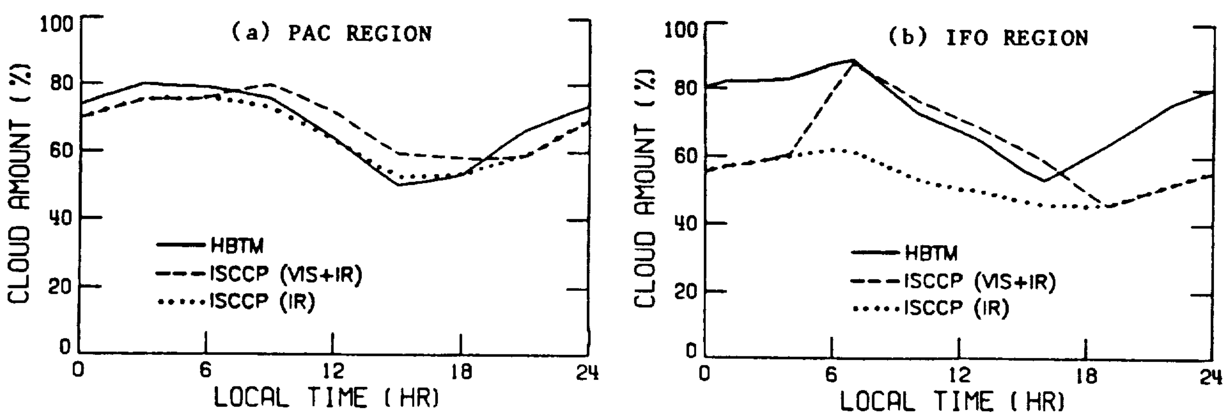


Fig. 4. Diurnal variations in mean total cloudiness for July 17-31, 1986.

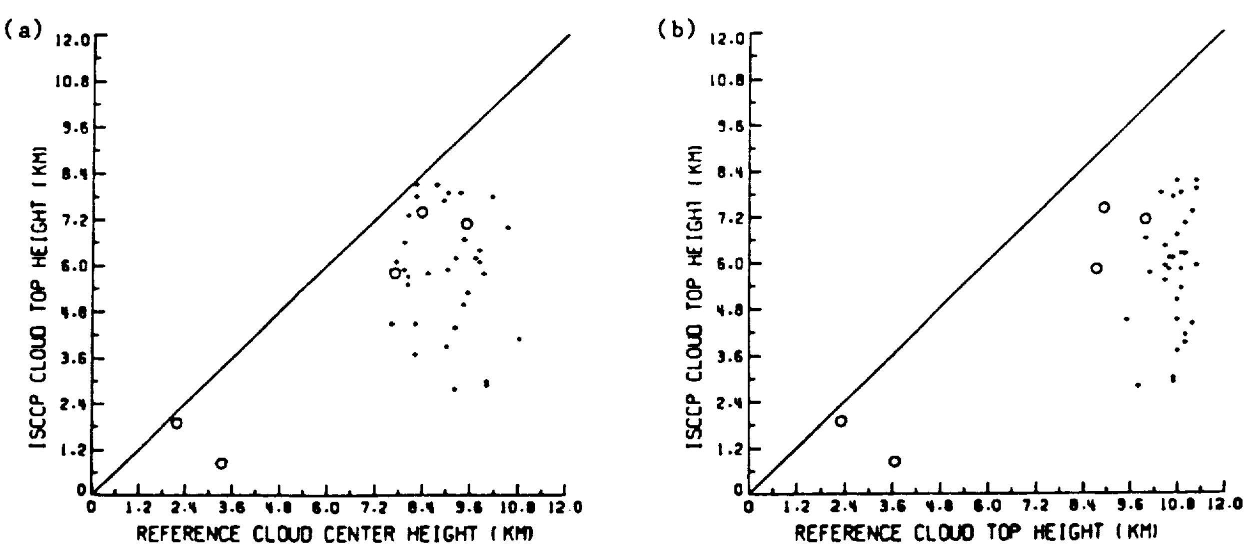


Fig. 5. Comparison of simulated and actual ISCCP cloud heights to reference data.